Diffraction by gratings

Toufic ABBOUD & Pedro FERREIRA

Centre de Mathématiques Appliquées

UMR CNRS 7641

École Polytechnique

Palaiseau

France

Outline

1. The 2-D Grating
   a) Geometry
   b) Maxwell equations, (TM) and (TE) modes
   c) Quasi-periodic solutions
   d) Fourier modes and radiation conditions
   e) The Dirichlet-to-Neumann Operator
   f) Properties of the Dirichlet-to-Neumann Operator
   g) Problem in the truncated domain
   h) Variational problem
   i) Main results
2. The curved grating

a) Geometry

b) Decomposition in quasi-periodic solutions

c) The truncated domain

d) Dirichlet-to-Neumann operator

e) Quasi-periodic solutions

f) Variational problem

g) Numerical example

3. Convex Gratings

a) Numerical example

4. Low frequency approximation

a) Example: on the (TM) case

b) Numerical results

1. Diffraction by an infinite 2D grating

a. Geometry

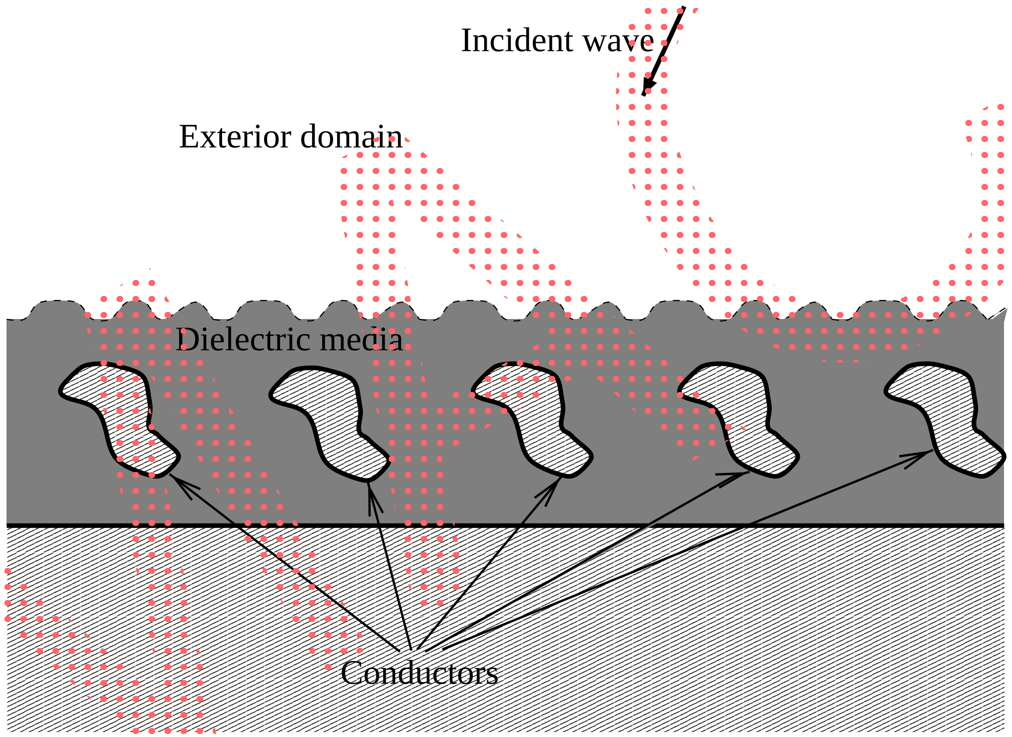

Figure 1: The infinite grating

- Ω^d is the dielectric medium;
- Ω^c the conducting medium;
- Ω^e the exterior domain;
- $\Omega = \mathbb{R}^2 \setminus \overline{\Omega^c}$

$\varepsilon_r : \Omega \longrightarrow \mathbb{C}$ relative electric permittivity.

and

$\mu_r : \Omega \longrightarrow \mathbb{C}$ relative magnetic permeability.

bounded periodic with the same period (d) as the grating.

In Ω^d :

$$\varepsilon_r(x_1, x_2) = \varepsilon'_r(x_1, x_2) + i\varepsilon''_r(x_1, x_2)$$

where :

$$0 < \varepsilon'_{\text{min}} \le \varepsilon'_r(x_1, x_2) \text{ and } 0 \le \varepsilon''_r(x_1, x_2)$$

$$\mu_r(x_1, x_2) = \mu'_r(x_1, x_2) + i\mu''_r(x_1, x_2)$$

where :

$$0 < \mu'_{\text{min}} \le \mu'_r(x_1, x_2) < \text{ and } 0 \le \mu''_r(x_1, x_2)$$

In Ω^e we have :

$$\varepsilon_r = \mu_r = 1$$

The grating is illuminated by an incident plane wave:

$$u^{\text{in}}(x_1, x_2) = e^{i\vec{k}\cdot\vec{x}}$$

b. Maxwell equations, (TM) and (TE) modes

(TM)
$$\begin{cases} \operatorname{div} \dfrac{1}{\mu_r} \nabla E_3 + \kappa^2 \varepsilon_r E_3 = 0 & \text{in } \Omega \\ E_3 = 0 & \text{in } \partial\Omega^c \\ E_3 - E_3^{\text{in}} \text{ satisfies a radiation condition} & \end{cases}$$

(TE)
$$\begin{cases} \operatorname{div} \dfrac{1}{\varepsilon_r} \nabla H_3 + \kappa^2 \mu_r H_3 = 0 & \text{in } \Omega \\ \dfrac{\partial H_3}{\partial n} = 0 & \text{in } \partial\Omega^c \\ H_3 - H_3^{\text{in}} \text{ satisfies a radiation condition} & \end{cases}$$

where $\kappa = \left|\vec{k}\right|$.

c. Quasi-periodic solutions

The incident wave verifies:

$$u^{\text{in}}(x_1 + jd, x_2) = u^{\text{in}}(x_1, x_2) e^{ijk_1 d}$$

i.e. it is k_1-quasi-periodic of period d.

Uniqueness issue leads to search for quasi-periodic solutions.

d. Fourier modes and radiation conditions

u admits the following Fourier expansion :

$$u(x_1, x_2) = \sum_{j \in \mathbb{Z}} u_j(x_2) e^{i\beta_j x_1}$$

where :

$$\beta_j = k_1 + j\frac{2\pi}{d}$$

and :

$$u_j(x_2) = \frac{1}{d}\int_0^d u(x_1, x_2) e^{-i\beta_j x_1}\, dx_1$$

The functions $u_j(x_2)$ satisfy :

$$u_j(x_2)'' + (\kappa^2 - \beta_j^2) u_j(x_2) = 0 \qquad x_2 > h$$

$$\kappa_j = \begin{cases} \sqrt{\kappa^2 - \beta_j^2} & \text{if } |\beta_j| < \kappa \\ i\sqrt{\beta_j^2 - \kappa^2} & \text{otherwise} \end{cases}$$

$$u_j(x_2) = u_j^+ e^{i\kappa_j x_2} + u_j^- e^{-i\kappa_j x_2}$$

Radiation condition: We choose outgoing and evanescent waves, then :

$$u_j^- = 0$$

e. The Dirichlet-to-Neumann Operator

On Γ_h u and $\frac{\partial u}{\partial n}$ are related by:

$$\left.\frac{\partial u^{\mathrm{d}}}{\partial n}\right|_{\Gamma_h} = T\left(u^{\mathrm{d}}|_{\Gamma_h}\right)$$

where:

$$T : \sum_{j\in\mathbb{Z}} u_j^0 e^{i\beta_j x_1} \longmapsto \sum_{j\in\mathbb{Z}} i\kappa_j u_j^0 e^{i\beta_j x_1}$$

$u^{\mathrm{d}} = u - u^{\mathrm{in}}$ is the diffracted wave.

f. Properties of the Dirichlet-to-Neumann Operator

- T is a pseudo-differential operator of order 1;
- T is a linear continuous operator from $H^s_{k_1}(\Gamma_h)$ to $H^{s-1}_{k_1}(\Gamma_h)$;
- T is non-local;
- If a quasi-periodic u satisfies $\Delta u + \kappa^2 u = 0$ for $x_2 > h$ and the radiation condition then :

$$\left.\frac{\partial u}{\partial n}\right|_{\Gamma_h} = T(u|_{\Gamma_h})$$

- Sign properties:

$$-\Re e \int_{\Gamma_h} T(u)\overline{u} \geq 0 \quad \forall u \in H^{\frac{1}{2}}_{k_1}(\Gamma_h)$$

$$\Im m \int_{\Gamma_h} T(u)\overline{u} > 0 \quad \forall u \in H^{\frac{1}{2}}_{k_1}(\Gamma_h)$$

g. Problem in the truncated domain

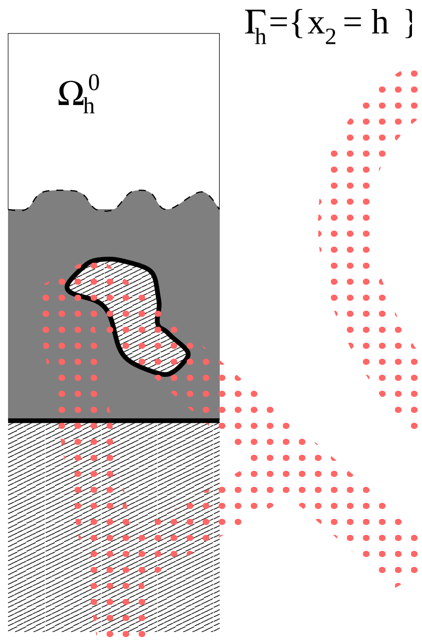

$$\Omega_h^0 = \Omega \cap \{0 < x_1 < d,\ x_2 < h\}$$

$$\Gamma^0 = \partial\Omega^c \cap \{0 < x_1 < d,\ x_2 < h\}$$

We search for quasi-periodic solutions of the systems:

$$\text{(TM)} \iff \begin{cases} \operatorname{div} \dfrac{1}{\mu_r} \nabla u + \kappa^2 \varepsilon_r u = 0 & \text{in } \Omega_h^0 \\ u = 0 & \text{in } \Gamma^0 \\ \dfrac{\partial}{\partial n}(u - u^{\text{in}}) = T(u - u^{\text{in}}) & \text{on } \Gamma_h \end{cases}$$

$$\text{(TE)} \iff \begin{cases} \operatorname{div} \dfrac{1}{\varepsilon_r} \nabla u + \kappa^2 \mu_r u = 0 & \text{in } \Omega_h^0 \\ \dfrac{\partial u}{\partial n} = 0 & \text{in } \Gamma^0 \\ \dfrac{\partial}{\partial n}(u - u^{\text{in}}) = T(u - u^{\text{in}}) & \text{on } \Gamma_h \end{cases}$$

h. Variational problem

$$\begin{cases} \text{find } u \in V \text{ such that } \forall v \in V \\ a(u,v) = L(v) \end{cases}$$

$$L(v) = \int_{\Gamma_h} \left(\frac{\partial u^{\text{in}}}{\partial n} - T(u^{\text{in}}) \right) \overline{v}$$

$$(\text{TM}) : \begin{cases} V = \left\{ v \in H^1_{k_1}(\Omega_h^0) \;:\; v = 0 \text{ on } \Gamma^0 \right\} \\ a(u,v) = \int_{\Omega_h^0} \frac{1}{\mu_r} \nabla u \cdot \nabla \overline{v} - \kappa^2 \int_{\Omega_h^0} \varepsilon_r u \overline{v} - \int_{\Gamma_h} T(u) \overline{v} \end{cases}$$

$$(\text{TE}) : \begin{cases} V = H^1_{k_1}(\Omega_h^0) \\ a(u,v) = \int_{\Omega_h^0} \frac{1}{\varepsilon_r} \nabla u \cdot \nabla \overline{v} - \kappa^2 \int_{\Omega_h^0} \mu_r u \overline{v} - \int_{\Gamma_h} T(u) \overline{v} \end{cases}$$

i. Main results

- Existence and uniqueness of solution except possibly for a discrete set, going to infinity, of frequencies.
- The variational approximation converges and we have classical results for finite element estimates. Error of truncation of the series defining T is exponentially small.

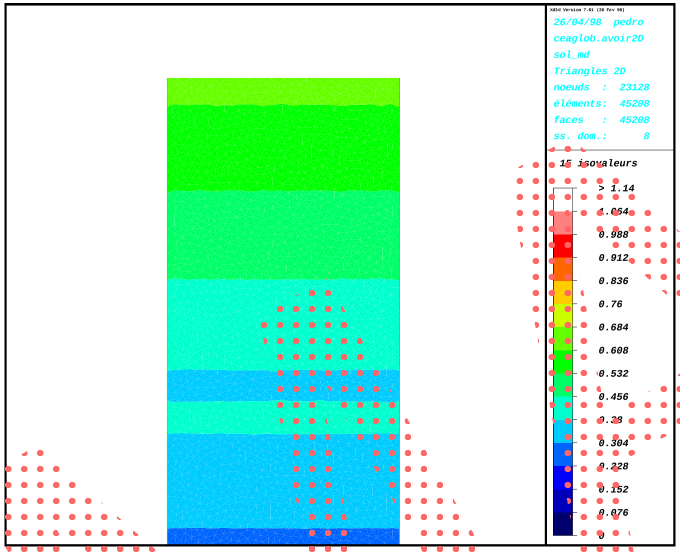

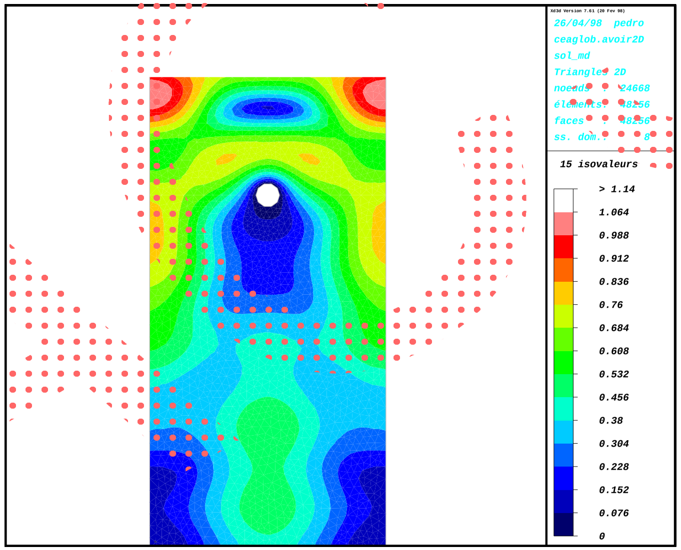

Figure 2: Comparison between homogeneous concrete and reinforced concrete

2. Diffraction by an finite curved 2D grating

a. Geometry

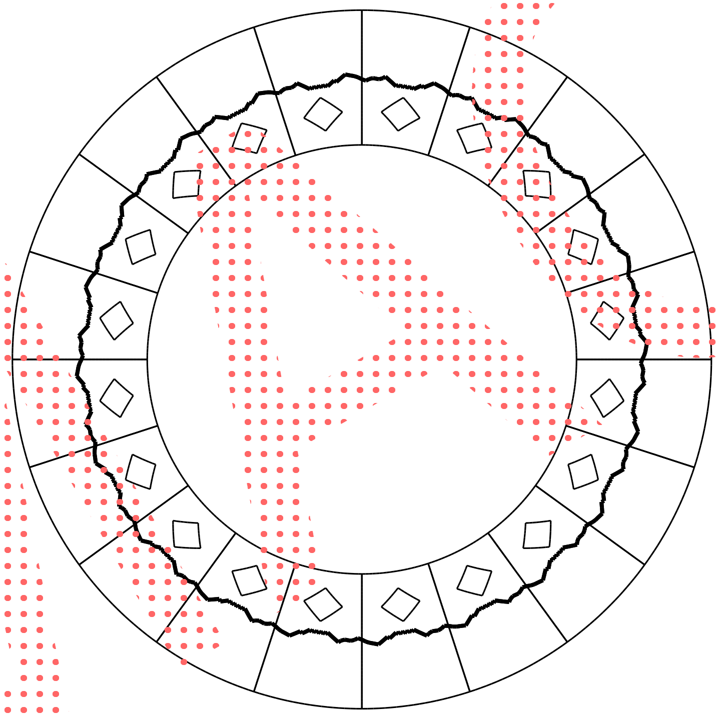

Figure 3: The finite circular grating

b. Decomposition in quasi-periodic solutions

$$u^{\text{in}} = \sum_{j=0}^{N-1} u_j^{\text{in}}$$

where

$$u_j^{\text{in}}(r,\theta) = \sum_{n\in\mathbb{Z}} u^{\text{in}}(r,\theta + n\frac{2\pi}{N})e^{-ijn\frac{2\pi}{N}}$$

u_j^{in} is quasi-periodic in θ:

$$u_j^{\text{in}}(r,\theta + \frac{2\pi}{N}) = u_j^{\text{in}}(r,\theta)e^{ij\frac{2\pi}{N}}$$

The solution u of the Helmholtz equation have the same decomposition:

$$u = \sum_{j=0}^{N-1} u_j$$

where each u_j is quasi-periodic.

c. The truncated domain

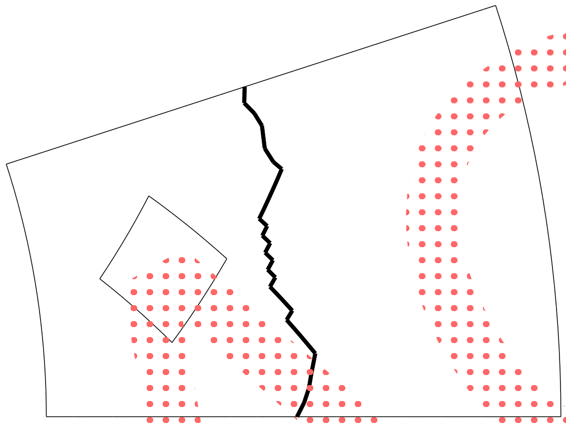

Figure 4: Truncated elementary cell

$$\Omega_R^0 = \Omega \cap \{0 < \theta < \tfrac{2\pi}{N},\ r < R\}$$

$$\Gamma^0 = \partial\Omega^c \cap \{0 < \theta < \tfrac{2\pi}{N},\ r < R\}$$

d. Dirichlet-to-Neumann operator

On $\Gamma_R^0 = \left\{0 < \theta < \frac{2\pi}{N}, r = R\right\}$ u_j and $\frac{\partial u_j}{\partial n}$ are related by the following relation:

$$\frac{\partial}{\partial n}\left(u_j - u_j^{\text{in}}\right)|_{\Gamma_R^0} = \mathcal{T}_j\left(u_j - u_j^{\text{in}}\right)|_{\Gamma_R^0}$$

$$\mathcal{T}_j \; : \; v = \sum_{p=nN+j, n\in\mathbb{Z}} u_p e^{ip\theta} \longmapsto \sum_{p=nN+j, n\in\mathbb{Z}} z_p u_p e^{ip\theta}$$

$$z_p = \kappa \frac{H_p^{(1)\prime}(\kappa R)}{H_p^{(1)}(\kappa R)}$$

$H_p^{(1)}$ is the Hankel function of order p satisfying the outgoing radiation condition.

e. Quasi-periodic solutions

We look for $j\frac{2\pi}{N}$-quasi-periodic u_j, such that:

$$\text{(TM)} \iff \begin{cases} \operatorname{div} \dfrac{1}{\mu_r} \nabla u_j + \kappa^2 \varepsilon_r u_j = 0 & \text{in } \Omega_R^0 \\ u_j = 0 & \text{in } \Gamma^0 \\ \dfrac{\partial}{\partial n}(u_j - u_j^{\text{in}}) = \mathcal{T}_j(u_j - u_j^{\text{in}}) & \text{on } \Gamma_R \end{cases}$$

$$\text{(TE)} \iff \begin{cases} \operatorname{div} \dfrac{1}{\varepsilon_r} \nabla u_j + \kappa^2 \mu_r u_j = 0 & \text{in } \Omega_R^0 \\ \dfrac{\partial u_j}{\partial n} = 0 & \text{in } \Gamma^0 \\ \dfrac{\partial}{\partial n}(u_j - u_j^{\text{in}}) = \mathcal{T}_j(u_j - u_j^{\text{in}}) & \text{on } \Gamma_R \end{cases}$$

f. Variational problem

$$\begin{cases} \text{find } u_j \in V_j \text{ such that } \forall v \in V_j \\ a_j(u_j, v) = L_j(v) \end{cases}$$

$$L_j(v) = \int_{\Gamma_R} \left(\frac{\partial u_j^{\text{in}}}{\partial n} - \mathcal{T}_j(u_j^{\text{in}}) \right) \overline{v}$$

$$\text{(TM)} : \begin{cases} V_j = \{ v \in H_j^1(\Omega_R^0) \ : \ v = 0 \text{ on } \Gamma^0 \} \\ a_j(u_j, v) = \int_{\Omega_R^0} \frac{1}{\mu_r} \nabla u_j \cdot \nabla \overline{v} - \kappa^2 \int_{\Omega_h^0} \varepsilon_r u_j \overline{v} - \int_{\Gamma_R} \mathcal{T}_j(u_j) \overline{v} \end{cases}$$

$$\text{(TE)} : \begin{cases} V_j = H_j^1(\Omega_R^0) \\ a_j(u_j, v) = \int_{\Omega_R^0} \frac{1}{\varepsilon_r} \nabla u_j \cdot \nabla \overline{v} - \kappa^2 \int_{\Omega_R^0} \mu_r u_j \overline{v} - \int_{\Gamma_R} \mathcal{T}_j(u_j) \overline{v} \end{cases}$$

g. Numerical example

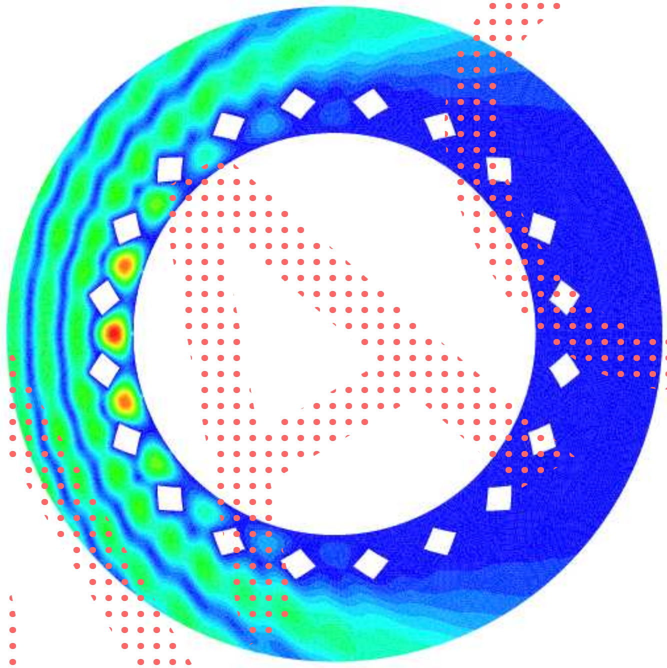

Figure 5: 20 periods, $\lambda = d$

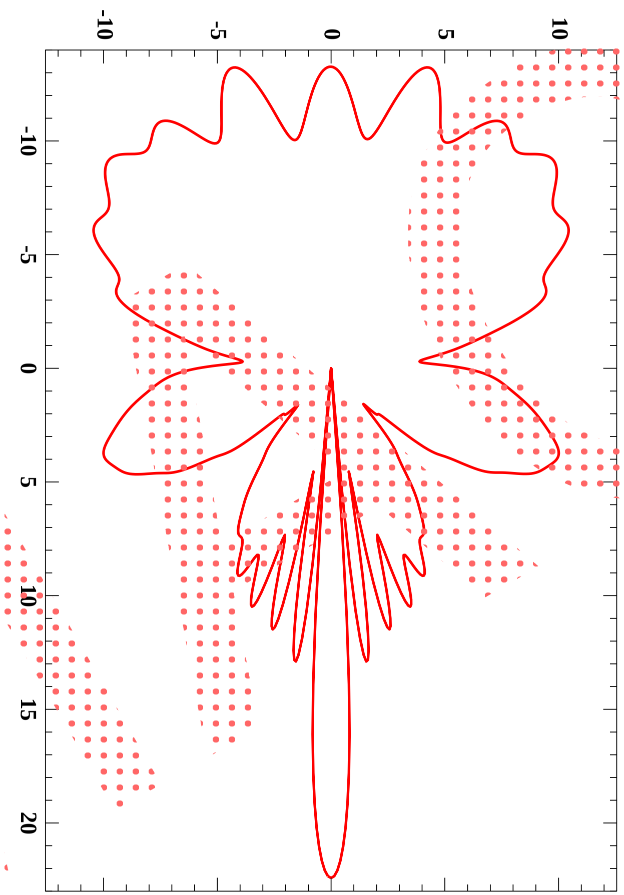

Figure 6: Directivity diagram, bi-static RCS

3. Asymptotic results for convex gratings

(T. Abboud, H. Ammari and G. Lebeau)

- Diffraction (TM) or (TE) by convex gratings at high frequencies: $\lambda = \frac{2\pi}{\kappa}$ of the same order as d.
- Outside transition regions they derived geometric optics solutions of arbitrary order.
- Transition regions :
  - Classical transition regions between light and shadow : grazing incident ray. Size : $O(\lambda^{1/3})$;
  - New transition regions : grazing diffracted ray, *i.e.* where some κ_j of the tangent infinite plane grating vanishes. Size : $O(\lambda^{2/3})$;
- Near the convex grating, outside the transition regions, the first order geometric optics approximation is the diffracted wave by the infinite plane tangent grating.

a. Numerical example

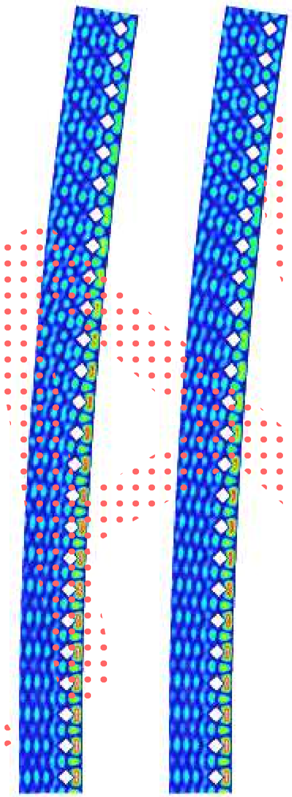

Figure 7: Exact and asymptotic solutions. 1000 periods, $\lambda = 0.555 \times d$

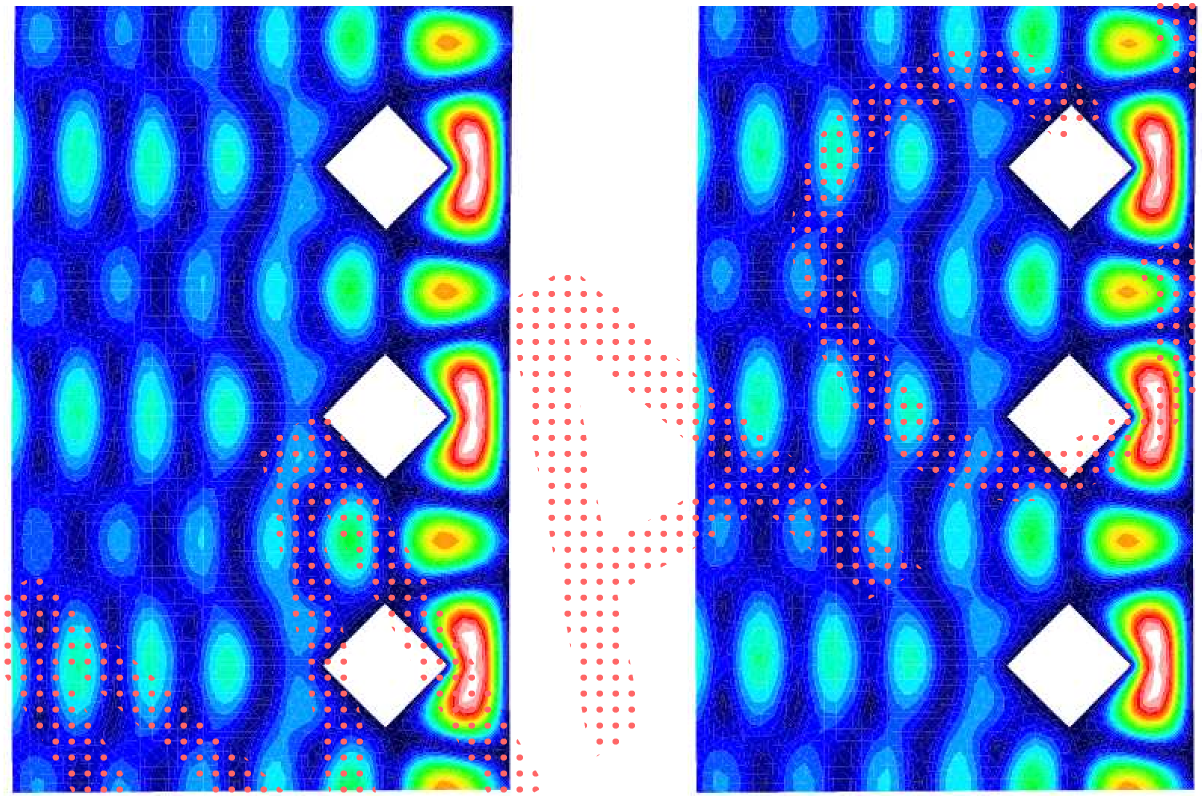

Figure 8: Exact and asymptotic solutions (zoom). 1000 periods, $\lambda = 0.555 \times d$

4. Low frequency approximation

(Y. Achdou, T. Abboud-H. Ammari)

- Diffraction of (TM) or (TE) waves by curved gratings at low frequencies: $\frac{d}{\lambda}$ small. λ may be small compared to the total obstacle.
- Asymptotic expansion with a boundary layer corrector and a total corrector.

a. Example: on the (TM) case

$$u^\delta = u^0 + u^0_{\text{BL}} + \delta\left(u^1 + u^1_{\text{BL}}\right) + \cdots$$

- u^0 is the field diffracted by the structure without the periodic layer;
- u^0_{BL} has the form:

$$u^0_{\text{BL}}(x) = \delta \frac{\partial u^0}{\partial n}(x_\Gamma)\left\{\alpha^{(0)}\left(\frac{s}{\delta}, \frac{n}{\delta}\right) - a^{(0)}\right\}$$

$$
\begin{cases}
\operatorname{div} \dfrac{1}{\mu_r^0} \nabla \alpha^{(0)} = 0 & \text{in } O^e \cup O^d, \\
\alpha^{(0)} = -y_2 & \text{on } G^c,\ \alpha^{(0)} = 0 \text{ on } G, \\
\left[\alpha^{(0)}\right] = 0,\ \left[\dfrac{1}{\mu_r^0} \dfrac{\partial \alpha^{(0)}}{\partial n}\right] = \left[-\dfrac{1}{\mu_r^0}\right] & \text{on } G^d \\
\alpha^{(0)} \to a^{(0)} & \text{as } y_2 \to \infty
\end{cases}
$$

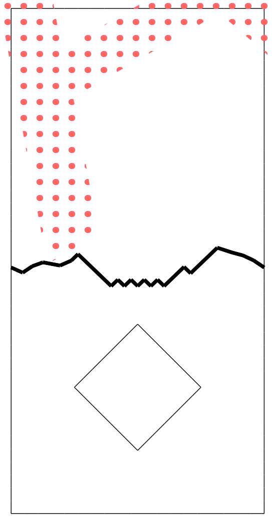

- u_1 is the solution of:

$$\begin{cases} \Delta u^1 + \kappa^2 u^1 = 0 & \text{in } \Omega, \\ u^1 = a^{(0)} \dfrac{\partial u^0}{\partial n} & \text{on } \Gamma, \\ u^1 \text{ satisfies the outgoing radiation condition} \end{cases}$$

- If we neglect the boundary layer the periodic layer is approximated in the order 1 by the following impedance condition:

$$\frac{\partial u^a}{\partial n} - d a^0 u^a = 0$$

- Curvature terms appear in the second order approximation.
- In the (TE) case curvature terms appear since the first order approximation.

b. Numerical results

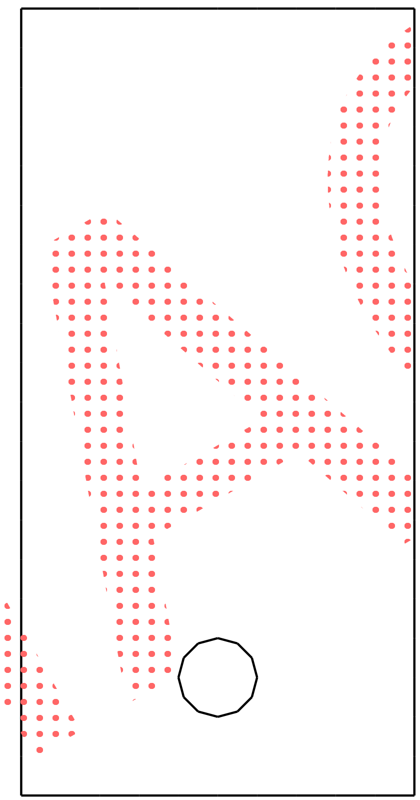

Figure 9: Elementary cell, circular conducting inclusion

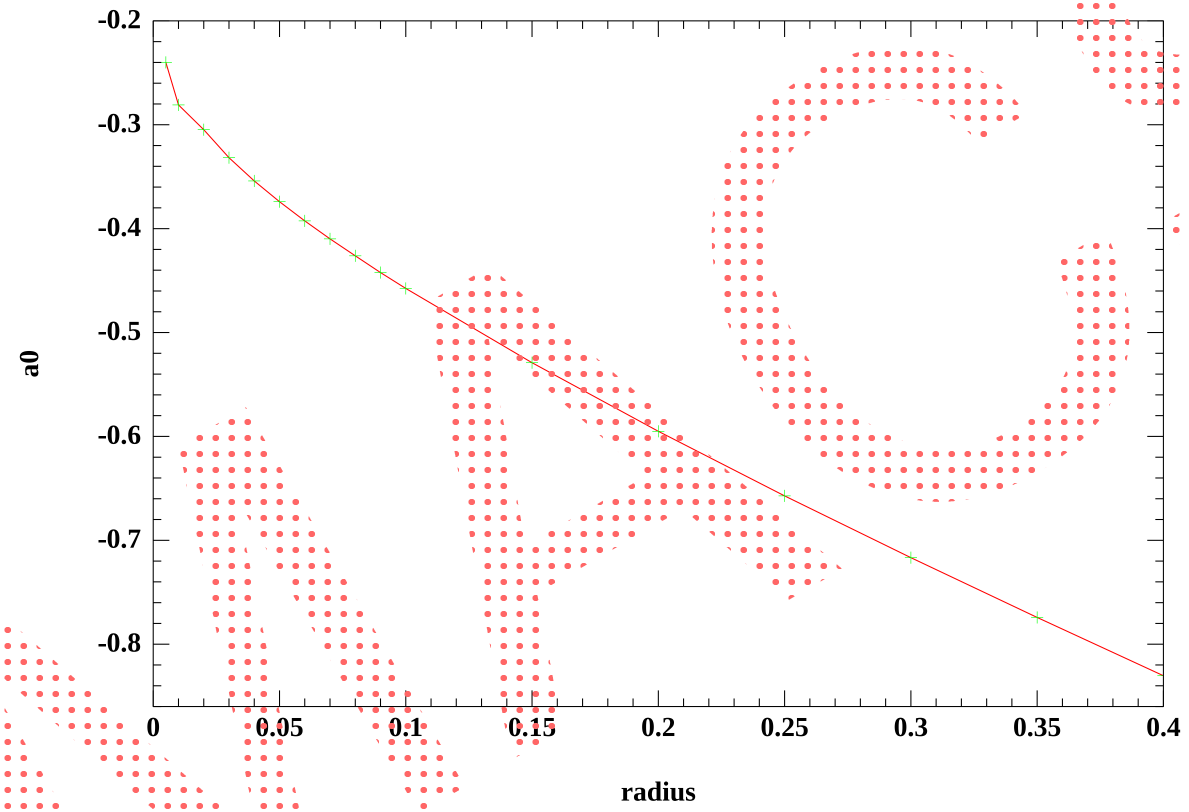

Figure 10: a^0 function of the radius of the disk

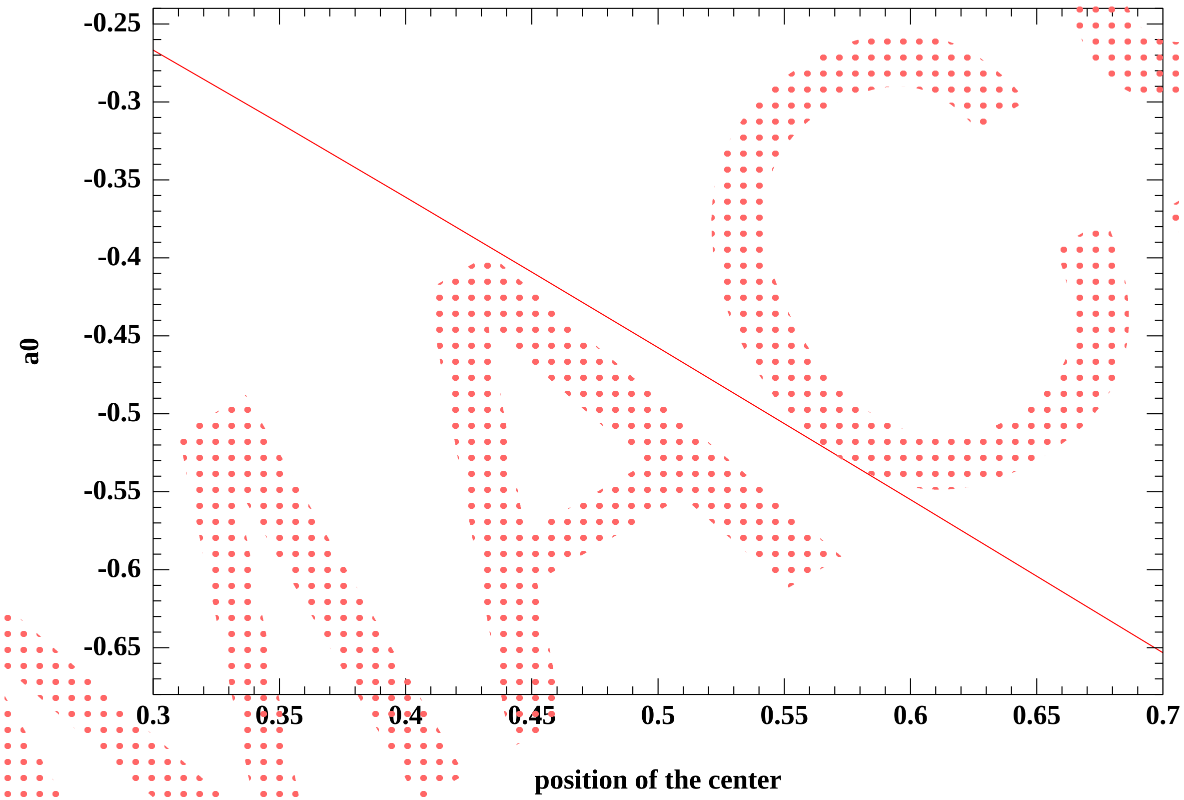

Figure 11: a^0 function of the center of the disk.

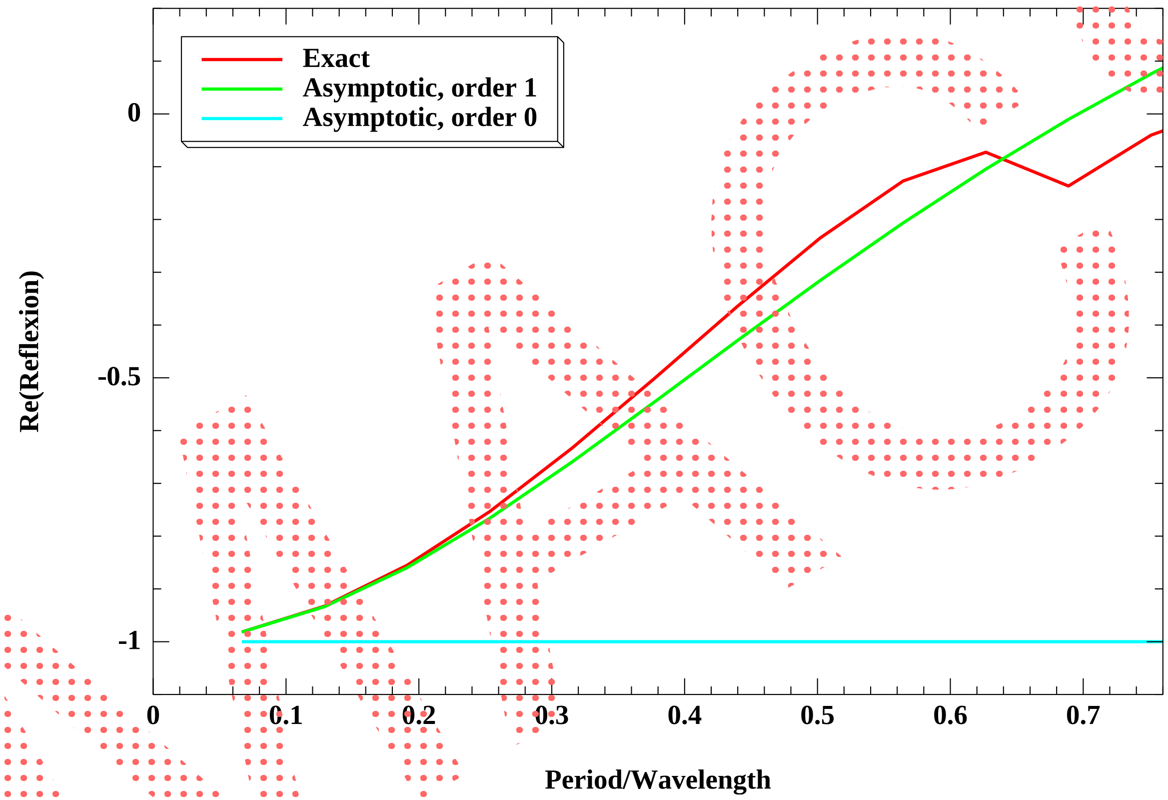

Figure 12: Real Part of the Reflection coefficient.

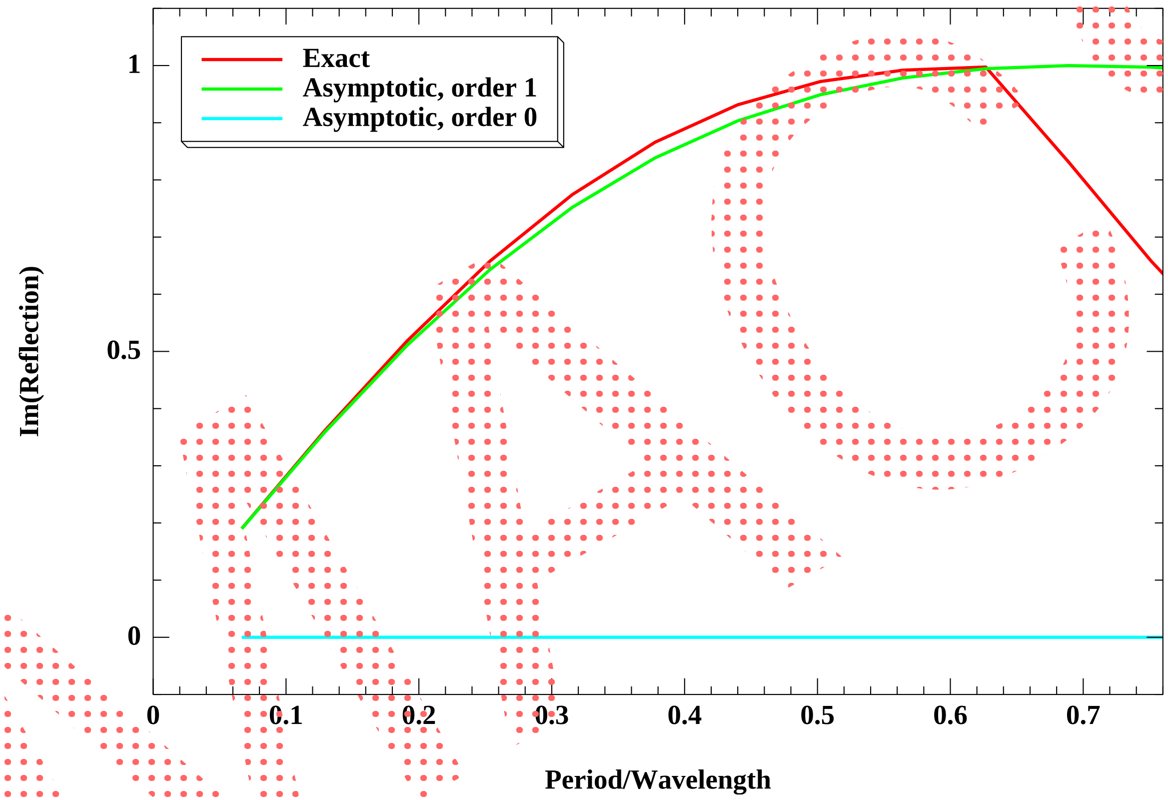

Figure 13: Imaginary Part of the Reflection coefficient.